Colloid Journal, Vol. 67, No. 4, 2005, pp. 469–477. Translated from Kolloidnyi Zhurnal, Vol. 67, No. 4, 2005, pp. 518–526.

The Effect of Fluid Properties on the Hydrodynamic Permeability Coefficient

I. A. Rodionova, E. I. Shkol'nikov, and V. V. Volkov

Topchiev Institute of Petrochemical Synthesis, Russian Academy of Sciences, Leninskii pr. 29, Moscow, 119931 Russia

Received December 29, 2004

Abstract—The effect of temperature (5–70°C), viscosity, and the nature of fluid on the hydrodynamic permeability (HDP) coefficient of inorganic ultrafiltration membranes was experimentally studied. The direct influence of fluid viscosity on the HDP coefficient within a high-temperature range, where this coefficient decreases with an increase in temperature, was established. A semiempirical expression for the HDP coefficient of a porous layer was proposed, which made it possible to interpret both monotonous and extremal dependences of the HDP coefficient on temperature for hydrophilic and hydrophobic porous media

INTRODUCTION

For predicting the filtration properties of porous membranes, it is necessary to understand the laws of flow of fluids through porous media and factors affecting their permeability coefficient. In spite of a long history of experimental and theoretical studies in this field [1, 2], the results of experimental measurements of the hydrodynamic permeability (HDP) coefficient of porous media still cannot be predicted from the data on the fluid viscosity and the structural characteristics of membranes. In theoretical approaches aimed at the establishment of a correlation between the HDP and the structure of porous media, the diverse methods of the porous medium modeling have been used [1–5]. Occasionally, new equations are derived which are usually have the empirical character and are applicable only to the porous medium of a particular type. Thus, the equations for porous media formed by a bimodal ensemble of particles [6], high-porous particles [7], and fibers [8] were derived. Specific equations were used to describe a high-porous medium [9], a porous medium with the structure deformed by the fluid flow [10], and a consolidated porous medium [11] which is generally characterized by a high tortuosity, as well as a porous medium with the wide or bimodal pore size distribution [11]. There are a few experimental works, in which the interrelation between the porous structure and permeability was studied. In our opinion, this is explained by significant difficulties in determining the structural parameters. Nevertheless, these studies are carried out regularly, because they are needed for solving the applied problems. For example, the experimental determination of structural parameters (mean pore size, porosity, and tortuosity) showed that the equation of type (1) (see below) can be applied to describe the flow process in a high-porous consolidated anisotropic medium (graphite) [12]. The direct temperature effect on the performance of porous membranes was revealed in [13, 14], and, in addition to the temperature effect, the influence of the fluid nature on the permeability of membranes with small pore size was established in [15].

FORMULATION OF THE PROBLEM

It is known that the laminar flow of liquid or gas in porous media under the pressure drop is described by the Darcy law, whereby the flow rate is proportional to the pressure drop on membrane, ΔP, and is inversely proportional to fluid viscosity η and membrane thickness L. The corresponding coefficient of proportionality, which is called the hydrodynamic permeability coefficient K is fully determined by the parameters of the porous structure, i.e., pore volume (porosity $\hat{\varepsilon}$), tortuosity τ, and, for a capillary model, by the integral mean-square pore radius $\bar{r}^2$ [1]

$$K = \frac{\hat{\varepsilon}\bar{r}^2}{8\tau} \quad (1)$$

or by the pore volume distribution over radii $\varepsilon(r)$ [16]

$$K = \frac{1}{8\tau}\int_0^{\hat{\varepsilon}} r^2 d\varepsilon. \quad (2)$$

In our opinion, to explain the discrepancy between the experimental values of K and their deviation from theoretical values, it is necessary to account for the factors affecting the fluid velocity profile but not directly related to the parameters of porous structure. Among these factors is the change in the structure of fluid layers adjacent to the solid surface compared to the bulk of fluid phase due to the effect of the field of surface forces [17, 18]. The introduction of the notion "structuring of fluid" contributed significantly to the study of the flow of fluids near interfaces [17–20]. Polar fluids with intermolecular hydrogen bonds, primarily water, are charac-

1061-933X/05/6704-0469

terized by strong and long-range changes in the structure. In the boundary layers of water, the structural changes manifest themselves by the variations in the density, the number and the energy of hydrogen bonds between molecules, and by the orientational ordering which is different near the hydrophilic and hydrophobic surfaces. In the first case, the dipoles of water molecules in boundary layers are predominantly oriented normally to the surface, the water density is higher, and the molecular mobility is lower compared to the bulk values that results in an increase in the effective viscosity of water in thin capillaries [17].

In the vicinity of the contact surface between water and hydrophobic phase (*n*-hexane, air, and hydrophobized quartz surface), the dipoles of water molecules are predominantly oriented in parallel to the surface. In this case, hydrogen bonds between water molecules are partially broken. The density of water in the boundary layer and its adhesion to the substrate are reduced due to the absence of hydrogen bonds between the hydrophobic wall and water molecules. As a result, the mobility of water molecules in the wall layers increases that can be interpreted as a macroscopic reduction in viscosity [18]. The latter fact can result also in the violation of the adherence boundary condition commonly used in hydrodynamics that makes it necessary, when solving hydrodynamic problems, to allow for the effect of fluid slip along the surface [19].

The viscosity of water in thin capillaries decreases with increasing temperature more sharply than the viscosity in the bulk due to the disruption of the specific structure of boundary layers under more intense thermal motion. At 65–70°C, the viscosity of water in thin capillaries is practically the same as the bulk viscosity [20]. The effect of thermal damage of the specific structure of water, which is exhibited in a higher flow velocity and a corresponding rise in the membrane performance was observed for fine-porous glasses [13] and track-etched filters [14]. An increase in the HDP coefficient with temperature was revealed also for fine-porous membranes made of silicon and zirconium oxides when studying the flow of methanol, ethanol, and propanol through these membranes [15].

Thus, the velocity of a fluid flow in pores is greatly dependent on the orientation of molecules in boundary layers, the presence of intermolecular bonds, and the ratio between the interaction forces of fluid molecules with each other and with the molecules of pore walls. To describe the effect of the change in the properties of a fluid near the solid surface on the general flow pattern in porous media, a microhydrodynamic approach must be used which relates transport coefficients not only to the structural specific features of porous bodies, but also to the physical properties of liquids and gases and the forces of molecular interaction with the pore surface.

Using non-Newtonian pseudoplastic fluids as an example, let us consider in terms of microhydrodynamic approach possible interpretation of the changes in the flow velocity profiles via the changes in the fluid properties. As is known, the flow of these fluids is accompanied by the orientation of asymmetric molecules with long axes parallel to the streamlines [21]. One of the distinguishing characteristics of the flow of such fluids is the specific velocity profile of their flow in a channel. It is much more uniform compared to the Poiseuille profile. In this case, the presence of a steeper profile in the near-wall region, where the mobility of a fluid in a narrow zone increases abruptly from zero to the maximal value, can be interpreted as a slip effect of the fluid. Such shape of the flow velocity profile results as a whole in a more efficient utilization of the channel volume compared to the case of the Poiseuille flow, which is characterized by a parabolic profile. Therefore, the channel permeability for a pseudoplastic fluid can be higher than for the Poiseuille fluid. The performance ratio for the channel utilization upon the flow of these fluids, in the limit, is equal to the ratio of the areas enveloped by the rectangle and parabola, i.e., 1 : 2/3.

To develop the microhydrodynamic approach, the direct determination of the velocity profiles is very useful [22]. In particular, these measurements demonstrated that, in the absence of polar molecules in a fluid, the most typical profile, even on well-wettable surfaces, is the profile that can correspond to the slipping plane of the fluid. Here, the slip effect is also related to the orientation of molecules along the flow axis that causes an increase in their mobility and a decrease in the fluid viscosity. In this case, the velocity profile is steeper compared to the Poiseuille profile, and the total flow velocity exceeds the velocity of Poiseuille flow. As follows from [22], the Poiseuille velocity profile is rather atypical case, which is realized under the conditions of the special purification of a fluid and the cleaning of metal surface.

In addition to the effect of the dynamic orientation of molecules, the velocity profile and the efficiency of channel utilization can be affected by the structuring of fluid near the solid boundary. The change in the mobility of a fluid can be interpreted as a macroscopic change in the HDP coefficient. The drag of a laminar ("creeping") flow of fluid through a porous medium can be reduced to the surface friction forces. By the summation of the friction forces over the whole of pore surface, the HDP coefficient was calculated as a function of the parameters of a porous medium and some other parameters affecting the interaction between the fluid and the pore surface [16]. The surface friction force includes the $(1 - \eta/\beta r)$ factor seemingly analogous to that used in the kinetic theory of gases when calculating the drag on a sphere moving in the gas in the hydrodynamic regime with slip, where β is the slip resistance coefficient [16]. The HDP coefficient expressed in the form, which is convenient for the processing of the cumulative curves of pore volume distribution over radii $\varepsilon(r)$, can be written as

$$K = \frac{1}{8\tau^2}\int_0^{\hat{\varepsilon}} \frac{r^2 d\varepsilon}{1-\eta/\beta r} \approx \frac{1}{8\tau^2}\frac{\hat{\varepsilon}\bar{r}^2}{1-\eta/\beta\bar{r}}. \quad (3)$$

The essence of concepts developed in this work on the basis of experimental data lies in the fact that, as the capillary diameter decreases and the fluid viscosity rises, the contribution of the effect of surface structuring to the total flow grows. As a result, with decreasing viscosity of the fluid, for example, due to an increase in temperature, the flow velocity does not increase in a strict proportion, as predicted by the Hagen–Poiseuille equation. On a macroscopic level, this discrepancy can be interpreted as a change in the permeability of porous medium, if the latter value is determined as a coefficient of proportionality in the Darcy law. Moreover, in some cases for glycerol in a specific temperature range, the typical deviation from the Darcy law was observed; i.e., upon the flow in pores, the Newtonian fluid acquired some features of pseudoplastic fluids.

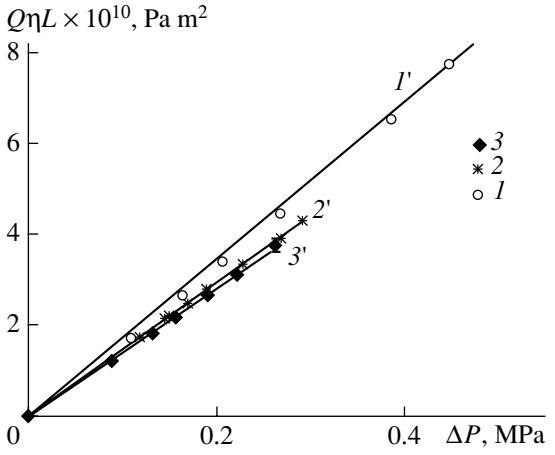

Fig. 1. Dependences of $Q\eta L$ on the pressure drop on the silicon carbide membrane for (*1*, *1'*) glycerol at 49°C, and Vaseline oil at (*2*, *2'*) 41.5 and (*3*, *3'*) 23°C. (*1'*–*3'*) are linear approximations obtained by the least squares method.

OBJECTS AND METHODS OF STUDY

In this work, plane symmetric inorganic membranes of two types, carbon membranes based on carbon black and membranes based on silicon carbide, kindly supplied by RNTS Prikladnaya Knimiya (Russian Scientific Center Applied Chemistry), were used as filtering elements. In addition, we used TRUMEM composite ultrafiltration membranes [23] where the selective layer 20 μm thick made of TiO_2/ZrO_2 was deposited onto a porous stainless steel with a pore diameter of about 2 μm. The TRUMEM membranes were used in the initial state after thermal treatment at 900°C in the helium atmosphere and the deposition of pyrocarbon formed upon the pyrolysis of methane [24, 25]. The radius of membrane pores was determined by dynamic desorption porosimetry [26]. The integral average radii of transport pores of a carbon and silicon carbide membranes were 55 and about 100 nm, respectively. The integral average radius of a TRUMEM membrane equal to 18 nm increased to 26 nm after thermal treatment and decreased to 20 nm after the pyrocarbon deposition.

The measurements of the HDP coefficient of the membranes were performed using the flow curves of model fluids through the membranes in a unit assembled according to a standard dead-end scheme of filtration experiments at different temperatures [16]. The sample diameter was 47 mm. The viscosity of fluids being studied was measured with a VPZh-3 capillary viscometer. The effect of pressure on viscosity was not taken into account because of the employed pressure range. For each temperature, the HDP coefficient was determined as a slope of the trend line for the experimental curve in the $Q\eta L$–ΔP coordinates, where Q is the volume flux and L is the thickness of a membrane or its selective layer (in the case of composite membranes) (Fig. 1). The linear character of the flow curve coming from the coordinate origin allows one to confirm the validity of the Darcy law along with the verification of methodological aspects. The method for calculating experimental error of the flow measurement is described in [16]. Figure 1 shows the set of flow curves for glycerol and Vaseline oil through the silicon carbide membrane. After the approximation of the experimental data by the linear function using the least squares method, the maximum deviation of the flow from the trend line was ±2% (Fig. 1) that coincides approximately with the calculated experimental error.

RESULTS

Figure 2 presents temperature dependences of HDP coefficients measured for polar and apolar model fluids with three TRUMEM membranes and a carbon membrane. As can be seen from Fig. 2, upon the filtration of ethanol through all membranes, the HDP coefficient grows with temperature that coincides with the analogous data for polar fluids [13–15]. In some cases of the flow of apolar liquids with a linear configuration of molecules (heptane, decane, and dodecane), the temperature dependence is absent, and in other cases, the tendency to decrease the HDP coefficient with temperature is observed, although the scope of this change remains within the measurement error. When decane flows through the initial TRUMEM membrane, the HDP coefficient decreases faster with temperature and exceeds the measurement error.

A more complex curve pattern was observed for high-viscosity liquids (glycerol and Vaseline oil). Figure 3 shows the temperature dependences of the HDP coefficient for the flow of decane, Vaseline oil, and glycerol through the silicon carbide membrane. For decane, the temperature dependence of K is qualitatively similar to the curves presented in Fig. 2. However, for more viscous fluids, the curves with maxima

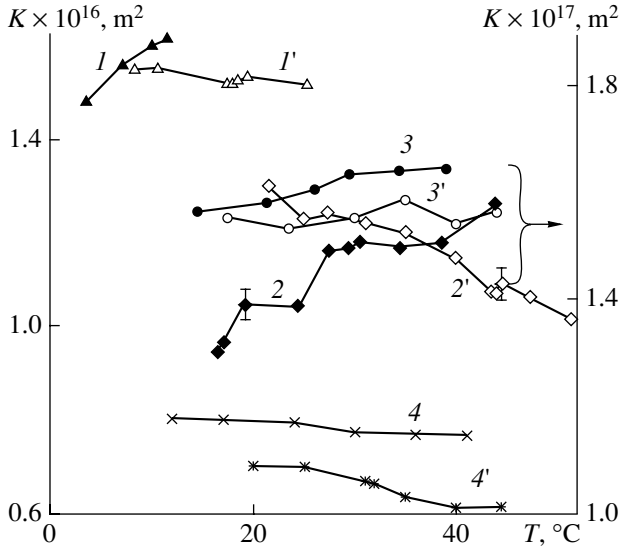

Fig. 2. Dependences of HDP coefficient on temperature for different membranes: (*1*) ethanol and (*1'*) heptane in carbon membrane; (*2*) ethanol and (*2'*) decane in the initial TRUMEM membrane; (*3*) ethanol and (*3'*) decane in TRUMEM membrane coated by pyrocarbon; (*4*) dodecane and (*4'*) decane in heated TRUMEM membrane.

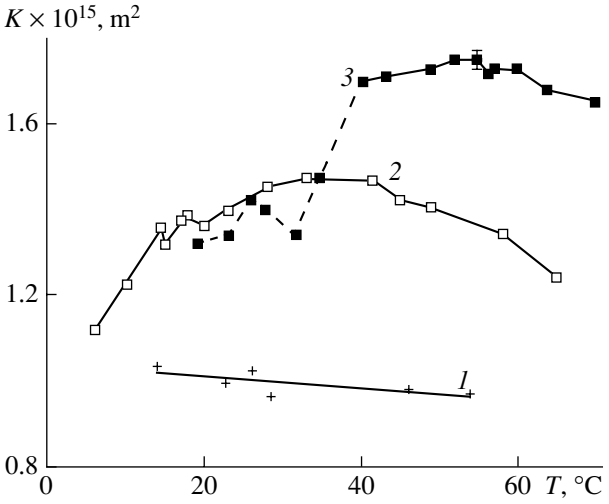

Fig. 3. Dependences of HDP coefficient on temperature for silicon carbide membrane with (*1*) decane, (*2*) Vaseline oil, and (*3*) glycerol.

are observed. Vaseline oil is apolar liquid with a composition difficult to be determined (State Standard GOST 3164-78). It is known [28] that the basic components of Vaseline oil comprise branched molecules that has an essential effect on its viscosity. The structuring of such fluids near the surface due to the presence of polar impurities extends to a significant distance and influences the flow velocity in narrow pores more strongly than the structuring of low-viscosity fluids. Thus, an increase in the HDP coefficient in the temperature range from 5 to 35°C could be explained by the disintegration of the spatial structure of Vaseline oil with temperature. Further drop in the HDP coefficient with increasing temperature can be attributed to a significant reduction in the viscosity that will be discussed below in more detail.

For glycerol in the temperature range of 40–70°C, the extremal dependence was also observed with the HDP coefficient exceeding the values measured for decane and Vaseline oil (Fig. 3). The K values first increase that is typical of polar fluids [13–15]. Further decrease in K with increased temperature was attributed to the reduced viscosity, as in the case of Vaseline oil. The temperature region below 40° will be considered further.

Experimental curves presented in Figs. 1–3 indicate that, for their interpretation, the allowance for the fluid structuring in pores and the corresponding change in the effective viscosity is insufficient. Temperature dependences of K (both monotone and extremal) must be explained using Eq. (3) obtained by the summation of fluxes in single pores, Q_i, which are determined by the modified Hagen–Poiseuille equation [16]

$$Q_i = \bar{v}\pi r_i^2 = \frac{\pi r_i^4}{8\eta\tau(1-\eta/\beta r_i)}\frac{\Delta P}{L}, \qquad (4)$$

where $\bar{v}$ is the average velocity in a pore. It follows from Eq. (3) that the common Hagen–Poiseuille equation corresponds to the limiting case of the minimal value of HDP coefficient K_0; the lower the viscosity of a fluid and the larger the pore radius, the greater the probability of this case to be realized.

With this approach, the β value is essentially a phenomenological parameter accounting for the structuring of fluid on the pore surface. Based on the analysis of the dimensionality and physical meaning of this parameter, one can suggest that it is proportional to the viscosity gradient in the surface zone calculated for the plane perpendicular to the surface. Then, the β parameter can be measured directly in special experiments, for example, similar to those described in [22].

In this work, the β parameter was calculated from the macroscopic flow velocity by the following scheme.

Let us write Eq. (3) in the dimensionless form

$$K = \frac{K_0}{1-S}, \qquad (5)$$

where K_0 characterizes the dependence of permeability on ε and τ, $S = \eta/\beta r$ is the cumulative dimensionless criterion characterizing the resultant effect of three parameters (bulk viscosity of fluid, its properties in boundary layers, and pore radius) on the flow velocity. Experimental data presented in Figs. 2 and 3 are summarized in Fig. 4 in accordance with the structure of Eq. (5). In this case, the minimal value of the HDP coefficient obtained for each membrane from the data for all fluids

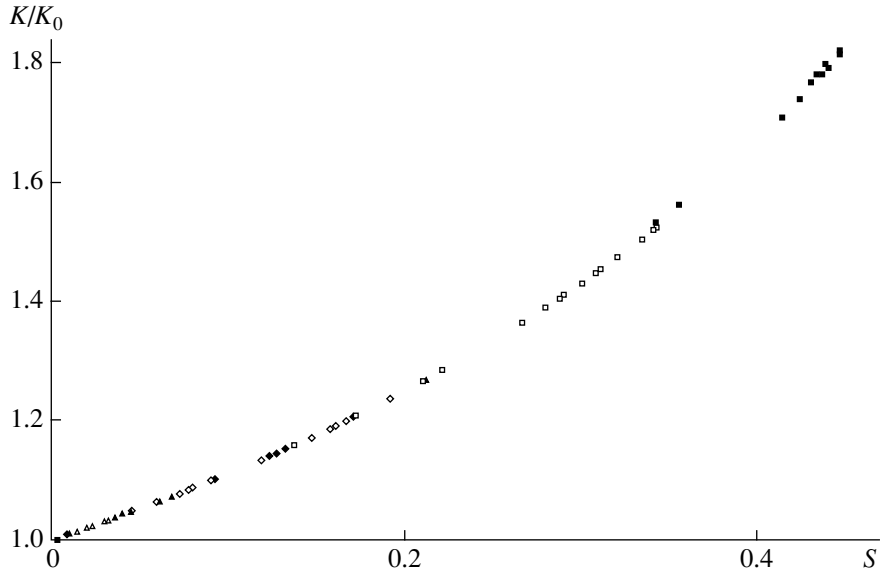

Fig. 4. Dependence of dimensionless HDP coefficient on criterion *S*. The designations are the same as in Figs. 2 and 3.

was taken as K_0. The resultant universal curve demonstrates clearly the effect of fluid structuring on the efficient utilization of the flow channel model and the order of *S* value. The universal character of this dependence could be confirmed by the independent determination of the β value; however, it is beyond the scope of this work.

Knowing the $\bar{r}$ value, one can calculate β by Eq. (5). Figure 5 presents the dependences of β on the viscosity of three fluids plotted by the data of Fig. 3 for the *K* values beginning with the highest temperature. As is seen from Fig. 5a, the points corresponding to experimental data lie initially on the same line irrespectively of the fluid type. For better illustration, the linear part of the curve is shown in Fig. 5b. The upward deviations of the curves from the line in Fig. 5a are caused by the structuring of fluids at low temperatures. Based on Fig. 5a, one can suggest that, for fluids much more viscous than water, the β value is determined by two contributions: "viscous" component β_μ related only to the fluid viscosity and "structural" component β_s due to the fluid structuring

$$\beta = \beta_\mu + \beta_s.$$

The equation of the line approximating linear dependence in Fig. 5b has the following form:

$$\beta_\mu = 0.0204\eta + 0.2632 \quad (6)$$

and makes it possible, for a specific membrane, to exclude β from Eq. (3) and to obtain the dependence of *K* on the viscosity of an arbitrary fluid, providing that the structuring in the studied temperature range is absent

$$K = \frac{0.965}{1 - \dfrac{\eta}{20.4\eta - 26.4}}. \quad (7)$$

The calculated dependence (the line in Fig. 6) is compared to the experimental curve plotted by the data of Fig. 3. Figure 6 shows that the calculated curve adequately fits the experimental points; however, it should be emphasized that this line is not their approximation. From the data in Fig. 6, we can estimate the range and scope of the effect of fluid viscosity on the efficient utilization of the flow channel model upon the flow that is not complicated by the structuring processes. The effect of viscosity is related to the leveling of the velocity profile that is observed with an increase in viscosity. As was shown above, this is the change in the velocity profile that is responsible for changes in the HDP coefficient of porous medium irrespectively of its nature.

The β_s parameter, which must be taken into account upon the fluid structuring, depends in a complicated manner on the fluid nature, the properties of interface, and temperature, i.e., it depends on the ratio between the forces of structuring and destructuring of a fluid. Figure 7 shows the experimental data for the β_s parameter as a function of temperature approximating the dependences for Vaseline oil and glycerol. These data, together with the temperature dependences of fluid viscosity [28], would allow for the better understanding of the mechanism of fluid structuring, as well as for a more precise determination of the scope of this effect.

It follows from Eq. (3) that, upon the temperature variations, the η and β values have opposite effects on *K*. Figure 8 shows the dependences of *K*, β, and *S* plotted from the data presented in Fig. 3, as well as the dependence of η on temperature for Vaseline oil. It is clearly

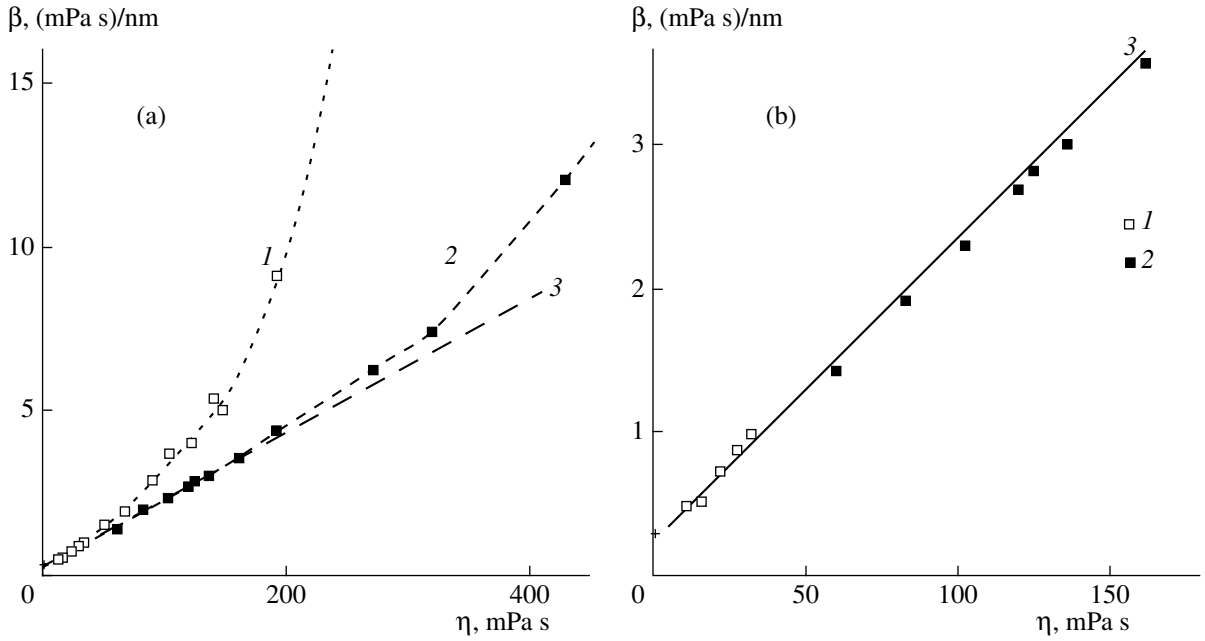

Fig. 5. Dependences of coefficient β on the viscosity for silicon carbide membrane at (a) low and (b) high temperatures: (*1*) Vaseline oil, (*2*) glycerol, and (*3*) dependence (6).

seen that, in the left-hand branch of the curve, K increases with temperature, because the β parameter decreases more rapidly than viscosity η. On the contrary, in the right-hand branch of the curve, K decreases, since, in this temperature range, viscosity η decreases more rapidly than the β parameter. On a microscopic level, the observed change in the K value suggests that, as temperature rises, the flow velocity profile is first expanded due to the initial large decline in the fluid structuring near the surface. Further increase in temperature tends to narrow the profile due to the weakening of viscous forces, which can no longer involve the adjacent surface layers of a fluid into the flow. For the quantitative estimation of the resultant effect of different factors including the pore radius, it is convenient to use dimensionless criterion S. The unambiguous dependence of K on S expressed by Eq. (5) (see Fig. 4) allows one to clearly explain the extremal character of the temperature dependence of K by the same character of the S dependence on temperature (see Fig. 8a).

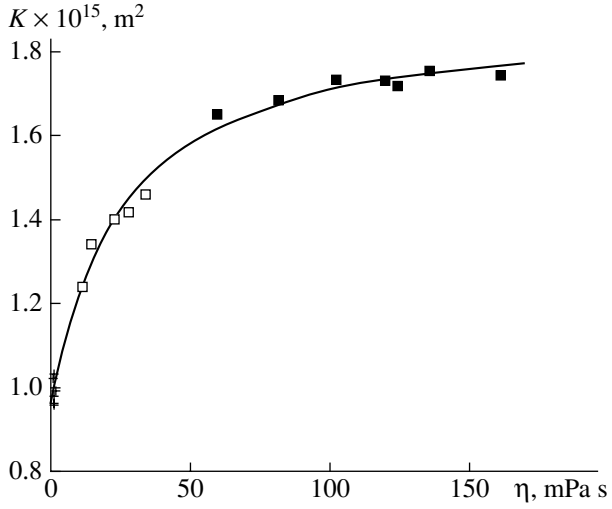

Fig. 6. Experimental and calculated dependences of HDP coefficient on the viscosity for silicon carbide membrane by the data of Fig. 3. See text for explanation.

The temperature dependences of K and S (Fig. 9) obtained for the flow of decane through two ceramic membranes with similar porous structures, but having different surface properties due to pyrocarbon deposited onto one of the membranes, illustrate rather clearly the effect of S on K. In the case of decane, it is unlikely that a decrease in K with temperature can be explained, on a microscopic level, by the drop in the η value, as was done for high-viscosity glycerol and Vaseline oil. In our opinion, at low temperatures, apolar linear molecules of decane located near the polar surface of oxide form a layered structure, where the molecules are oriented along the flow axis in parallel to the pore surface [22]. Evidently, this phenomenon tends to increase the mobility of boundary layers of the fluid compared to the case of a random orientation of molecules at high temperatures. When the surface is coated with pyrocarbon, the dominant orientation of molecules seemingly is not observed.

For the flow of ethanol through the same membranes (see Fig. 2, curves *2* and *3*), the opposite situation takes place. The molecules of polar fluid in the proximity to polar surface are predominantly oriented

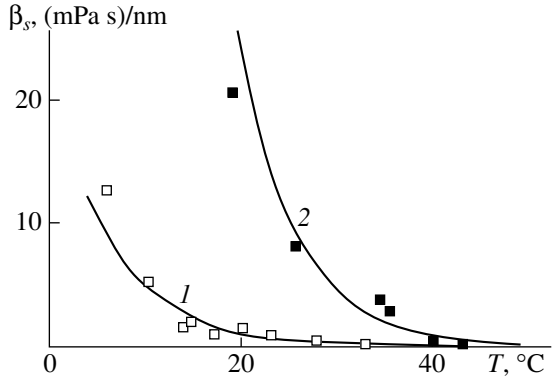

Fig. 7. Dependences of coefficient β_s on temperature for silicon carbide membrane: (*1*) Vaseline oil and (*2*) glycerol. The approximating dependences and correlation coefficients are as follows: (*1*) $\beta_s = 21.817e^{-0.148T}$, $R^2 = 0.9755$; (*2*) $\beta_s = 647.87e^{-0.164T}$, $R^2 = 0.964$.

perpendicularly to the flow axis, thus sharply decreasing the flow velocity in the boundary layers. It is evident that, as temperature increases, the contribution of the structuring effects lowers also for polar fluids. On the pore surface coated with pyrocarbon, the polar interaction is fairly weak and the effect of structuring is less pronounced, thus correspondingly affecting the temperature dependence of the HDP coefficient.

In conclusion, let us return to the most ambiguous result, the temperature dependence of the HDP coefficient for glycerol (Fig. 3, curve *3*). The HDP coefficient changes nonmonotonously in the region of 30°C. We believe that this result is due to the disclosed deviation from the Darcy law upon the flow of glycerol (Newtonian fluid) through the pores of a silicon carbide membrane at temperatures below 40°C. For three experimental curves presented in Fig. 10, the trend lines used for determining the K values at 26 and 40.1°C adequately fit the experimental points, and, at 31.7°C, the trend line is clearly different than the experimental curve. Hence, the formally correct determination of the HDP coefficient by the slope of trend line is erroneous (therefore, in Fig. 3, the points on the curve for glycerol at $T < 40$°C are connected by the dotted line).

The similarity in the behavior of glycerol and pseudoplastic fluid in pores can be also interpreted in terms of microhydrodynamic approach. It is well known [18, p. 76] that the deviations from the Darcy law observed for fluids in real porous bodies with a rigid skeleton can be caused by the differences in the rheological properties of a filtering fluid and Newtonian fluids due to the presence of colloidal particles or polymer molecules forming three-dimensional structures. A similar effect can supposedly be caused by the structuring of glycerol molecules near the surface due to polar interactions whose range is extended far from the surface. The disintegration of the glycerol boundary layers occurs not only with an increase in temperature as in the case of water, but also under the shear stresses arising due to higher flow velocity with an increase in pressure. At relatively low temperatures, the velocity of glycerol is so low and the boundary layers are still sufficiently strong to conserve their structure throughout the range of studied pressures; hence, the linear character of the flow curve remains practically unchanged. An increase in temperature tends to weaken the bonds between molecules. As a result, for low ΔP, the structure of boundary layers is conserved, and, as the flow velocity increases, the molecules in boundary layers are oriented along the streamlines. This results in the effect illustrated in Fig. 10, namely, the existence of the tem-

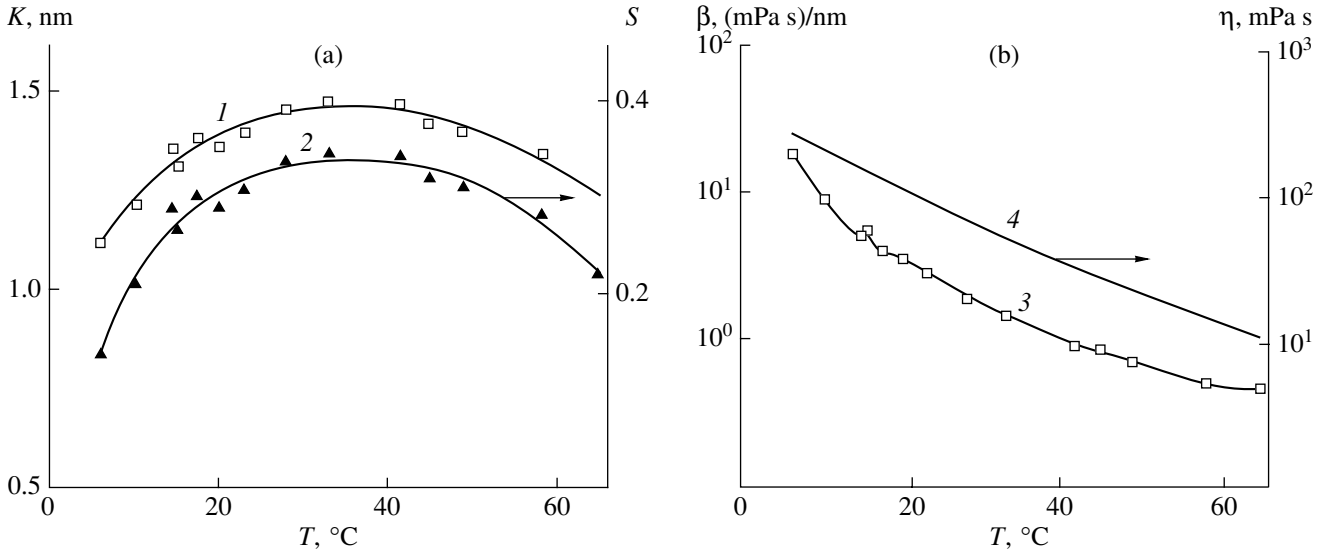

Fig. 8. Temperature dependences of different parameters for Vaseline oil–silicon carbide membrane system: (*1*) K, (*2*) S, (*3*) β, and (*4*) η.

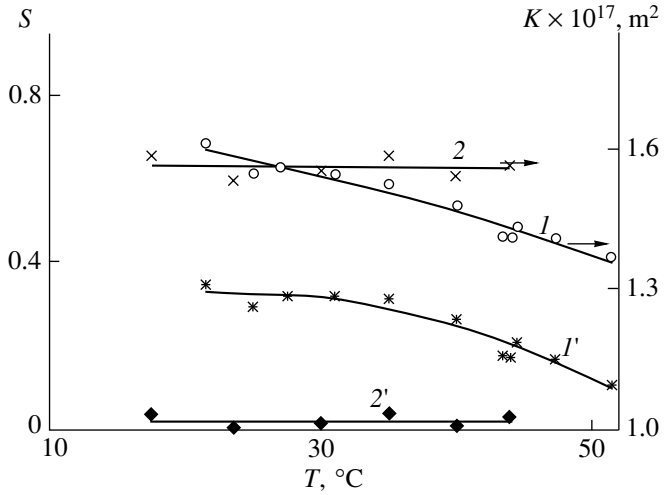

Fig. 9. Temperature dependences of K and S for decane in (*1*) the initial TRUMEM membrane and (*2*) TRUMEM membrane coated by pyrocarbon.

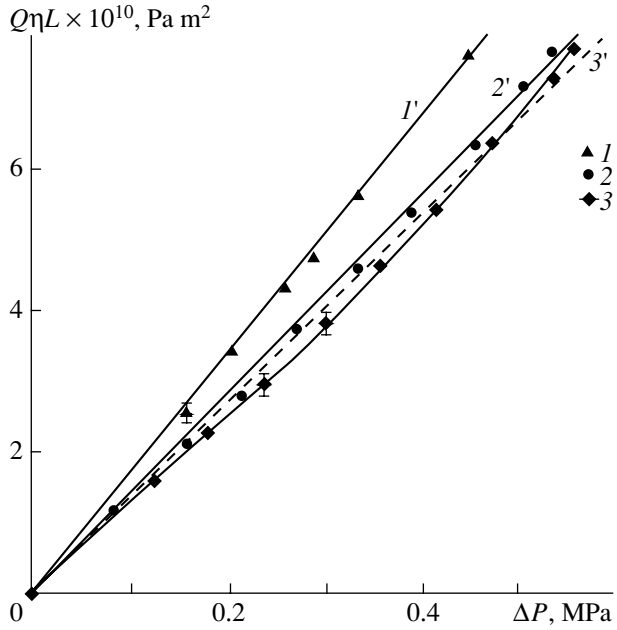

Fig. 10. Dependences of $Q\eta L$ value on the pressure drop on silicon carbide membrane for glycerol at (*1*, *1'*) 40.4, (*2*, *2'*) 26, and (*3*, *3'*) 31.7°C. (*1'*–*3'*) are linear approximations obtained by the least squares method.

perature range where the Darcy law is violated upon the flow of glycerol in porous body. These violations disappear at 40°C and the deviations from the trend line fall again within the limits of the measurement error.

CONCLUSIONS

The phenomenological approach described in this work made it possible to explain all the obtained experimental dependences including the deterioration of the rheological properties of the fluid in pores. In some cases, we were fortunate to derive the relations, which allow us to quantitatively predict the behavior of membrane HDP coefficient depending on the fluid viscosity and the pore radius of membranes.

ACKNOWLEDGMENTS

This work was supported by the Russian Foundation for Basic Research, project no. 03-03-32103.

REFERENCES

1. Scheidegger, A.E., *Fizika techeniya zhidkostei cherez poristye sredy* (The Physics of Flow of Fluids through Porous Media), Moscow: GNTINL, 1960.
2. Katz, A.J. and Thompson, A.H., *Phys. Rev. B: Condens. Matter,* 1986, vol. 34, p. 8176.
3. Chi-Ok Hwang, Given, J.A., and Mascagni, M., *Phys. Fluids,* 2000, vol. 12, no. 1, p. 7.
4. Xu, K., Daian, J.-F., and Quenard, D., *Transp. Porous Media*, 1997, vol. 26, p. 319.
5. Dasgupta, R., Shashwaty, R., and Tarafdar, S., *Physica A* (Amsterdam), 2000, vol. 275, no. 1, p. 22.
6. Macdonald, M.J., Chu, C.F., Guilloit, P.P., and Ng, K.M., *AIChE J.*, 1991, vol. 37, no. 10, p. 1583.
7. Pfeiffer, J.F., Chen, J.C., and Hsu, J.T., *AIChE J.*, 1996, vol. 42, no. 4, p. 932.
8. Ducket, K.E., Cain, I., Krowicki, R.S., and Thibodeaux, D.P., *Text. Res. J.*, 1991, vol. 61, no. 6, p. 309.
9. Rahli, O., Tadris, L., Miscevic, M., and Santini, R., *J. Phys. II*, 1995, vol. 5, no. 11, p. 1735.
10. Kamst, G.F., Bruinsma, O.S.L., and De Graauw, J., *AIChE J.*, 1997, vol. 43, no. 3, p. 673.
11. Bao, Y. and Evans, J.R.G., *J. Eur. Ceram. Soc.*, 1991, vol. 8, no. 2, p. 81.
12. Mauran, S., Rigaud, L., and Coudevylle, O., *Transp. Porous Media*, 2001, vol. 43, no. 3, p. 355.
13. Khadakhane, N.E., Sobolev, V.D., and Churaev, N.V., *Kolloidn. Zh.*, 1980, vol. 42, no. 5, p. 911.
14. Apel', P.Yu., Kolikov, V.M., and Kuznetsov, V.Ya., *Kolloidn. Zh.*, 1985, vol. 47, no. 4, p. 772.
15. Toshinori, T., Takashi, S., Tomohisa, Y., and Masashi, A., *J. Colloid Interface Sci.*, 2000, vol. 228, no. 2, p. 292.
16. Shkol'nikov, E.I., Kovtunov, S.N., and Volkov, V.V., *Kolloidn. Zh.*, 1996, vol. 58, no. 4, p. 553.
17. Churaev, N.V., *Kolloidn. Zh.*, 1996, vol. 58, no. 6, p. 725.
18. Churaev, N.V., *Fiziko-khimiya protsessov massoperenosa v poristykh telakh* (Physical Chemistry of Mass Transfer in Porous Media), Moscow: Khimiya, 1990.

19. Churaev, N.V., Sobolev, V.D., and Somov, A.N., *J. Colloid Interface Sci.*, 1984, vol. 97, no. 2, p. 574.

20. Zorin, Z.M., Sobolev, V.D., and Churaev, N.V., *Dokl. Akad. Nauk SSSR*, 1970, vol. 193, no. 4, p. 630.

21. Wilkinson, W., *Non-Newtonian Fluids. Fluid Mechanics, Mixing and Heat Transfer*, London, 1960.

22. Derjaguin, B.V. and Karasev, V.V., *Zh. Fiz. Khim.*, 1959, vol. 33, no. 1, p. 100.

23. Trusov, L., *Int. Newsletter Membr. Technol.*, 2000, no. 128, p. 10.

24. Shkol'nikov, E.I., Rodionova, I.A., Soldatov, A.P., *et al.*, *Zh. Fiz. Khim.*, 2004, no. 5, p. 943.

25. Soldatov, A.P., Shkol'nikov, E.I., Rogailin, M.I., *et al.*, *Zh. Fiz. Khim.*, 2004, no. 9, p. 1659.

26. Shkol'nikov, E.I. and Volkov, V.V., *Dokl. Ross. Akad. Nauk*, 2001, vol. 378, no. 4, p. 507.

27. *Kratkaya khimicheskaya entsiklopediya* (Abridged Chemical Encyclopedia), Moscow: Sovetskaya Entsiklopediya, 1961, vol. 1.

28. Frenkel, Ya.I., *Kineticheskaya teoriya zhidkostei* (Kinetic Theory of Fluids), Moscow–Leningrad: Akad. Nauk SSSR, 1959.